J. Chem. Sci. Vol. 126, No. 3, May 2014, pp. 547–559.

Glyoxylate as a reducing agent for manganese(III) in salen scaffold: A kinetics and mechanistic study

AKSHAYA K KAR[a], ACHYUTANANDA ACHARYA[b], GURU C PRADHAN[a] and ANADI C DASH[a,*]

[a]Department of Chemistry, Utkal University, Bhubaneswar 751 004, India
[b]Department of Chemistry, College of Engineering and Technology, Bhubaneswar 751 003, India
e-mail: aacharya@cet.edu.in; gurucpradhan@yahoo.co.in; acdash1@rediffmail.com

MS received 27 August 2013; revised 4 December 2013; accepted 7 December 2013

Abstract. The kinetics of oxidation of glyoxylic acid (HGl) by $Mn^{III}(salen)(OH_2)_2^+$ ((H_2salen = N,N′-bis(salicylidene)ethane-1,2-diamine) is investigated at 30.0–45.0°C, 1.83 ≤ pH ≤ 6.10, I = 0.3 mol $dm^{-3}(NaClO_4)$. The products are identified as formic acid, CO_2 and Mn^{II} with the reaction stoichiometry, $|\Delta[Mn^{III}]/\Delta[HGl]| = 2$. The overall reaction involves fast equilibrium pre-association of $Mn^{III}(salen)(OH_2)_2^+$ with HGl and its conjugate base Gl^- forming the corresponding inner sphere complexes (both HGl and Gl^- being the monohydrate gem-diol forms) followed by the slow electron transfer steps. In addition, the second order electron transfer reactions involving the inner-sphere complexes and HGl/Gl^- are also observed. The rate, equilibrium constants and activation parameters for various steps are presented. $Mn^{III}(salen)(OH_2)(Gl)$ is virtually inert to intra molecular electron transfer while the process is facile for $Mn^{III}(salen)(OH_2)(HGl)^+$ (10^5k_{et} = 2.8 ± 0.3 s^{-1} at 35.0°C) reflecting the involvement of proton coupled electron transfer mechanism in the latter case. A computational study of the structure optimization of the complexes, trans-$Mn^{III}(salen)(OH_2)_2^+$, *trans*-$Mn^{III}(salen)(OH_2)(Gl)$, and *trans*- $Mn^{III}(salen)(OH_2)(HGl)^+$ (all high spin $Mn^{III}(d^4)$ systems), reveals strongest axial distortion for the (aqua)(Gl) complex ; HGl bound to Mn^{III} centre by the C=O function of the carboxyl group in the (aqua)(HGl) complex facilitates the formation of a hydrogen bond between the proton of the carboxyl group and the coordinated phenoxide moiety ((O-H. . .O hydrogen bond distance 1.745 Å) and the gem-diols are not involved in H-bonding in either case. A rate comparison for the second order paths: $Mn^{III}(salen)(OH_2)(HGl)/Gl)^{+/0}$+ HGl/$Gl^-$ → products, shows that HGl for the (aqua)(HGl) complex is a better reducing agent than Gl^- for the (aqua)(Gl) complex (k_{HG} ~ 5 k_{Gl}). The high values of activation enthalpy ($\Delta H^{\neq}$ = 93–119 kJ mol^{-1}) are indicative of substantial reorganization of the bonds as expected for inner-sphere ET process.

Keywords. Glyoxylate; Mn^{III}(salen); electron transfer; kinetics; DFT.

1. Introduction

Manganese is known to exist in different formal oxidation states ranging from −I to +VII. Note worthy is the fact that it is an essential catalyst in +III and +IV oxidation states in the Nature's tetra manganese cluster of the oxygen evolving system (OEC) of photosystem II (PS II) available in Plants' domain; the involved catalytic water splitting reaction entails redox cycling of Mn^{IV} and Mn^{III}.[1–4] Recently a novel binuclear Mn^{III} complex, $[Mn_2^{III,III}(tpdm)_2(\mu\text{-}O)(\mu\text{-}OAc_2)]^{2+}$ (tmpd = *tris*(2-pyridyl)methane) has been modelled as Nature's water oxidation catalyst.[5] However, there is little success in this regard. The Mn^{III}(salen) (H_2salen = N,N′-*bis*(salicylidene)ethane-1,2-diamine) and several similar complexes, in their SOD and catalase mimicry, undergo redox cycling of Mn^{III} and Mn^{II} states, get transformed to the oxo-Mn^{IV} species under oxidative stress and implicated as possible therapeutic agents for neurodegenerative conditions in Alzheimer's, and Parkinson's diseases and multiple sclerosis.[6] Several enzymes in which Mn is a cofactor are also well-known and the importance of this metal ion in +II state on human physiology has been well-recognized.[7] Though an essential element it is also a potential toxicant at high concentration level causing degeneration of neurons in brain even in +II state and more so in higher oxidation states.[8] The redox sensitivity of this metal ion in higher oxidation states has been exploited in several synthetic and limited kinetics studies in the past.[9] However, every new complex formed by Mn in +III/IV state offers challenges in respect of understanding the mechanistic aspects of reactions with reducing/oxidizing agents as rates and paths of reactions are likely to be

*For correspondence

characteristic features of the reacting partners.[9] We have been investigating the redox and ligand substitution reactions of Mn^{III}/Mn^{IV} species keeping that in mind.[10,11] In that context, we report here a detailed and elaborate study of the kinetics and mechanism of the reaction of Mn^{III}(salen) with glyoxylate, a reductant of considerable importance due to its involvement in glycine catabolism[12] and plant physiology.[13] To the best of our knowledge there is no report of this work earlier, although similar works are available in the literature for the sake of comparison.

2. Experimental

2.1 *Materials and reagents*

Mn^{III}(salen)Cl,H_2O was prepared by the published method essentially as described by Sharpe and coworkers except that LiCl was used in place of KCl.[14,6d] The elemental analysis was in satisfactory agreement with this formulation. IR (cm^{-1}, KBr): 1598.4(C=N), 1292.8(C-O of the phenoxide moiety), 3394 (OH of H_2O). Similar observation was also made by Banerjee *et al.*[15] for $[Mn^{III}(salen)ClH_2O]H_2O$ (vC=N, 1598; vC-O, 1286; vOH, 3404–3448 cm^{-1}); for $Mn^{III}(salen)(OH_2)_2^+$ (generated *in situ*, pH 4, aqueous medium) λ_{max}, nm (ε, $dm^3\ mol^{-1}\ cm^{-1}$): 234.8 (40,243), 279 (18,625); lit.[15]: 234 (37, 600), 279 (17,100). Glyoxylic acid monohydrate, HGl (AR, Sigma Aldrich, purity 98%) was used without further purification. The concentration of the acid in the stock solution was further checked by potentiometric titration using standard NaOH. All other reagents were AR grade. Water was doubly distilled. The second distillation was made from alkaline $KMnO_4$ in a standard joint fitted borosilicate glass distillation apparatus. Freshly distilled water was used to prepare solutions for kinetic runs. The stock solution of the complex (5×10^{-3} mol dm^{-3}) was protected from light and stored in a refrigerator at ~20°C. Ionic strength adjustment was done with $NaClO_4$ which was prepared by mixing standard solutions of NaOH and $HClO_4$ in requisite volumes. The pH of the stock $NaClO_4$ solution was adjusted to 6 and the concentration checked by a combined ion-exchange alkalimetric procedure using Dowex 50W X8 resin in the H^+ form.[16]

2.2 *Physical measurements*

A Systronics (India) model 118, and a Perkin Elmer Lambda 25 UV-visible spectrophotometers with a matched pair 10 mm quartz cells were used for all absorbance measurements. The I R measurements were made on a Perkin Elmer FTIR spectrometer, model Spectrum 2 using KBr pellet. ESR measurement was performed on a JEOL (Japan) JES-FA 200 ESR spectrometer at room temperature operating in X-band mode (8.75–9.65 GHz, power 1.08 W, sensitivity 7×10^9 spins/0.1 mT, resolution 2.35 μT). The mass spectrum of the Mn^{III} complex (aqueous solution) was recorded on a Macromass Q-TOF ESI-MS mass spectrometer. The pH measurements were made with a Systronics (India) pH meter model 335 using a glass-Ag/AgCl, Cl^- (3 mol dm^{-3} NaCl) electrode CL 51. NBS buffers of pH 4.01, 6.86 and 9.20 prepared from KHphthalate, Na_2HPO_4/ KH_2PO_4, and $Na_2B_4O_7$, $10H_2O$, respectively were used to calibrate the pH meter. The measured pH of the reaction medium was converted to $p[H^+]$ (= -log$[H^+]$) by the relationship $p[H^+] = (1.09 \pm 0.02)pH - 0.318 \pm 0.075$ established by a calibration curve using dilute $HClO_4$ solutions ($1.98 \times 10^{-2} \leq [H^+]$ / mol $dm^{-3} \leq 1.00 \times 10^{-5}$).[17]

2.3 *Kinetics*

The rate measurements were made by batch sampling technique under pseudo first order conditions at $30.0 \leq t$, °C ≤ 45.0. The reaction mixture containing all components except the complex was equilibrated in a 50 or 100 cm^3 measuring flask in a water thermostat maintained at the desired temperature (±0.1°C). The complex solution was also thermally equilibrated separately. It may be noted that the complex, $Mn^{III}(salen)(OH_2)Cl$, instantaneously aquates[10] to $[Mn^{III}(salen)(OH_2)_2]^+$ (m/z+ : 392.97(obs), 392.79 (cal) for $[Mn(salen)(OH_2)_2,Cl]$) and hence the reaction we studied is the reaction of the di-aqua complex with glyoxylate. After thermal equilibrium was reached, a known volume of the complex (1 cm^3) was quickly transferred in to the reaction mixture and volume was made up. Samples (5 cm^3) were withdrawn from the reaction mixture in to a clean and dry test tube kept at 10°C to quench the reaction by cooling. Immediately absorbance (A) was measured at 280 nm against solvent blank. The concentration of the complex, $[Mn^{III}(salen)(OH_2)_2]^+$ was varied as $(3–6) \times 10^{-5}$ and that of $[Gl]_T$ (= total glyoxylic acid concentration) in the range of 0.001–0.1 mol dm^{-3}. The ionic strength of the medium was fixed at 0.3 mol dm^{-3} ($NaClO_4$) unless otherwise quoted. The ionic strength variation, to examine the effect of ionic back ground on rate, was made in the range of 0.01–0.4 mol dm^{-3} at 40°C, constant pH (=2.21 ± 0.05) and $[complex]_T$ ($=2.805 \times 10^{-5}$ mol dm^{-3}). The pH of the reaction mixture varied in the range of 1.83–6.10 by self-buffering due to glyoxylic acid/glyoxylate which

could be achieved by addition of standard solution of $NaOH/HClO_4$ to glyoxylic acid solution.

The observed rate constants (k_{obs}) were calculated by fitting the absorbance (A_t) – time (t) data to equation (1)

$$A_t = (A_0 - A_\infty) \exp(-k_{obs} t) + A_\infty. \quad (1)$$

A_∞ was close to zero for the completion of the reaction which was further verified by simulating the reaction mixture at complete reaction with appropriate solutions made out of Mn^{II} acetate, glyoxylic acid and other components at the same pH. The initial absorbance was in the range of 0.5–0.8. For very slow reactions ($k_{obs} \sim 10^{-5}$–10^{-6} s^{-1}) the rate constants were evaluated by the method of initial rate. In this case A_t - time(t) data were fitted to equation (2), a limiting form of equation (1),

$$A_t = C' \exp(-k_{obs} t) = C' - C' k_{obs} t, \quad (2)$$

where $C' = A_0[1 - (A_\infty/A_0)]/\left[1 - (A_\infty/A_t)\right]$ (for $A_t \sim A_0$ and $A_\infty \sim 0$, $C' \to A_0$); $\sigma(k_{obs})/k_{obs}$ from data fitted to equation (1) was generally better than ±2% while the same to equation (2) was ±6%. The rate data are presented in tables 1 and 2.

2.4 *Product analysis and stoichiometry*

The batches of reaction mixtures of Mn^{III}(salen) + excess HGl at different pHs (1.8–2.5) were set aside at 40°C till the brown colour of the complex was fully discharged ($10t_{1/2}$) indicating complete reduction of Mn^{III}. The unreacted HGl was then estimated by the method of Kramer *et al.*[18] which involved the formation of a pink coloured formazan derivative of HGl using phenyl hydrazine and $K_3Fe(CN)_6$ and measuring absorbance at 520 nm ($\varepsilon_{520\ nm}$ = 17870 dm^3 mol^{-1} cm^{-1}). The details of the procedure adopted has been described by Nayak and co-workers.[19] Our

Table 1. Rate data forthe reduction of Mn^{III}(salen)$(OH2)_2^+$ by Glyoxalate (Gly) at 30.0° and 35.0°C.[a]

$[Gly]_T$/ mol dm^{-3}	pH[a]	$10^5 k_{obs}/s^{-1}$	$10^5 k_{cal}/s^{-1}$	$[Gly]_T$/mol dm^{-3}	pH[a]	$10^5 k_{obs}/s^{-1}$	$10^5 k_{cal}/s^{-1}$
30.0 ± 0.1°C				35.0 ± 0.1°C			
0.001	2.38	0.076	0.033	0.001	2.36	0.086	0.048
0.004	2.30	0.14	0.15	0.004	2.34	0.25	0.21
0.007	2.28	0.23	0.28	0.007	2.30	0.44	0.39
0.010	2.23	0.44	0.44	0.010	2.27	0.77	0.58
				0.010	3.06	0.31	0.31
				0.010	3.00	0.55	0.33
0.015	2.18	0.51	0.74	0.020	2.11	1.07	1.39
0.020	2.15	1.07	1.07	0.020	2.23	1.11	1.33
0.025	2.15	0.98	1.42	0.030	2.06	2.18	2.30
0.025	2.11	0.94	1.44	0.030	2.96	1.24	1.19
				0.035	3.10	1.20	1.20
0.030	2.11	1.87	1.81	0.040	2.02	3.18	3.30
0.040	2.07	3.03	2.65	0.050	1.98	4.39	4.37
0.050	2.02	4.30	3.57	0.060	1.96	5.82	5.47
0.060	2.05	4.51	4.42	0.060	2.08	5.06	5.27
0.080	1.98	6.77	6.45	0.080	2.01	7.24	7.79
0.100	1.97	7.77	8.46	0.100	1.97	10.1	9.95
0.080	1.98	6.11	6.45	0.020	1.83	1.80	1.48
0.100	1.95	8.94	8.52	0.020	2.23	1.40	1.33
0.020	3.00	0.32	0.48	0.020	2.72	1.03	0.98
				0.020	2.90	0.85	0.81
0.020	3.09	0.35	0.43	0.020	3.21	0.65	0.56
0.020	3.20	0.31	0.36	0.020	3.30	0.55	0.50
0.020	3.49	0.26	0.24	0.020	3.42	0.56	0.43
0.020	3.63	0.24	0.21	0.020	3.56	0.46	0.37
0.020	3.89	0.17	0.17	0.020	3.74	0.33	0.32
0.020	4.18	0.22	0.16	0.020	4.00	0.200	0.27
0.020	5.16	0.14	0.14	0.020	4.51	0.15	0.23
				0.020	5.20	0.14	0.22
				0.020	6.00	0.21	0.22

[a] $\boldsymbol{I}$ = 0.3 mol dm^{-3}; -log$[H^+]$ = 1.09 pH - 0.318

Table 2. Rate data for the reduction of $Mn^{III}(salen)(OH_2)_2^+$ by Glyoxalate (Gly) at 40.0°C and 45.0°C.[a]

$[Gly]_T$/mol dm^{-3}	pH[a]	10^5k_{obs}/s^{-1}	10^5k_{cal}/s^{-1}	$[Gly]_T$/mol dm^{-3}	pH[a]	10^5k_{obs}/s^{-1}	10^5k_{cal}/s^{-1}
40.0 ± 0.1°C				45.0 ± 0.1°C			
0.001	2.36	0.084	0.052	0.001	2.38	0.15	0.055
0.004	2.83	0.21	0.23	0.004	2.33	0.44	0.25
0.007	2.29	0.45	0.42	0.007	2.30	0.66	0.49
0.010	2.25	0.65	0.66	0.010	2.23	1.03	0.79
0.015	2.16	1.06	1.11	0.015	2.18	1.41	1.38
0.020	2.13	1.39	1.60	0.020	2.16	2.06	2.06
0.020	2.15	1.30	1.60	0.025	2.12	2.72	2.87
0.025	2.10	2.47	2.14	0.030	2.10	3.34	3.75
0.030	2.10	2.36	2.71	0.040	2.05	4.31	5.80
0.030	2.08	3.37	2.73	0.050	2.05	8.34	8.03
				0.05	2.12	7.63	7.80
0.040	2.04	4.03	4.03	0.060	2.00	11.6	10.7
0.040	2.05	3.69	4.02	0.080	1.98	17.2	16.3
0.050	2.01	5.57	5.46	0.080	2.01	15.8	16.1
0.050	2.01	5.59	5.46	0.100	1.95	22.2	22.6
0.060	1.99	6.82	6.99	0.020	2.67	1.45	1.48
0.080	1.97	10.1	10.2	0.020	2.78	1.44	1.33
0.100	1.93	14.4	13.9	0.020	2.90	1.42	1.18
0.100	1.90	13.6	14.0	0.020	3.00	1.35	1.05
0.020	2.72	1.12	1.08	0.020	3.07	1.16	0.98
0.020	2.76	1.02	1.04	0.020	3.14	1.11	0.91
0.020	2.90	0.97	0.89	0.020	3.33	0.97	0.78
0.020	2.98	0.88	0.81	0.020	3.53	0.85	0.70
0.020	3.05	0.88	0.78	0.020	3.71	0.75	0.66
0.020	3.14	0.80	0.68	0.020	3.85	0.75	0.65
0.020	3.63	0.55	0.45	0.020	4.00	0.67	0.65
0.020	3.82	0.45	0.42	0.020	4.10	0.68	0.65
0.020	3.94	0.35	0.41	0.020	4.28	0.59	0.65
0.020	4.63	0.33	0.39	0.020	4.39	0.50	0.65
0.020	6.13	0.29	0.39	0.020	4.79	0.44	0.65
				0.020	5.34	0.43	0.65

[a] Same as under table 1

result, $-\Delta[HGL]/-\Delta[Mn^{III}(salen)] = 1.99 \pm 0.08$, indicated that the average consumption of Mn^{III} per mol of HGl was 2. The product manganese species was Mn^{II} ($I_N = 5/2$) as evidenced from the 6 line ESR spectrum of the spent reaction mixture (see figure 1).

The other products of oxidation are formic acid and CO_2; the former was established qualitatively by chromotropic acid test[20,21] and the latter by precipitating as a white solid by $CaCl_2$ under ammoniacal condition and performing the conventional test for CO_2 on treatment with dilute HCl. Accordingly the overall stoichiometry of the reaction of glyoxylic acid monohydrate ($CH(OH)_2CO_2H$) in acidic medium is given by equation (3).

$$2Mn^{III}(salen)(OH_2)_2^+ + CH(OH)_2CO_2H = 2Mn^{II}(salen)(OH_2)_2 + HCO_2H + CO_2 + 2H^+. \quad (3)$$

2.5 *Test of free radical*

The reaction carried out at pH = 2.08 (adjusted with $HClO_4$) with $[HGl]_T = 0.03$, $[Mn^{III}(salen)]_T = 2.805 \times 10^{-5}$, $I = 0.3$ mol dm^{-3}, 40°C in the presence of $[acrylamide]_T = 0.0$, 0.01, 0.02, and 0.03 mol dm^{-3} yielded 10^5k_{obs}/s^{-1} as 2.25, 1.90, 1.73, and 1.61, respectively. This small decreasing trend of k_{obs} distinctly shows the involvement of a radical intermediate from glyoxylic acid which reacted with $Mn^{III}(salen)$ almost instantaneously to maintain the stoichiometry as shown in equation (3) but was scavenged by acrylamide causing a decrease in the overall rate constant (k_{obs}). However, the competitive effectiveness of acrylamide in influencing the radical scavenging was not so significant under these experimental conditions as we did not observe any polymer formation in contrast to the polymerization of this monomer in acidic medium by the redox couple HGL + Mn^{IV} complex reported by Nayak *et al.*[19]

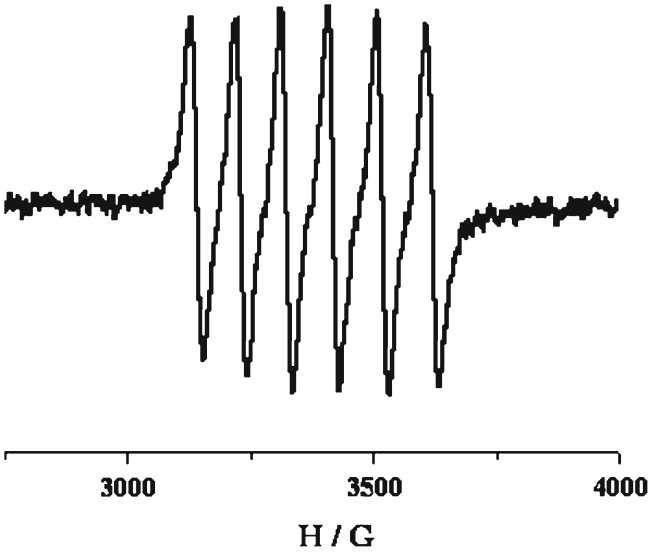

Figure 1. Six line ESR spectrum of the product manganese(II) in solution of $Mn^{III}(salen)(OH_2)_2^+$ + HGl after completion of the reaction. Intensity versus H/G (Gauss) plot at room temperature; g = 2.028, hyperfine constant a = 95.8 G.

3. Results and discussion

3.1 *Preliminary observations*

Figure 2 displays the repetitive spectral scans of the reaction mixture ($250 \leq \lambda$, nm ≤ 500 nm) at 40°C, pH = 2.05 over extended time. There is a steady decrease of absorbance at all wavelengths with an isosbestic point at 265 nm. The final spectrum (curve 12) shows a maximum at 322 nm which corresponds to that of a freshly prepared solution of Mn^{II}+ glyoxylic acid + H_2salen under similar conditions (except that the simulated solution is 2% v/v MeOH/water as methanolic solution of H_2salen is used). Hence the spectral behaviour is in conformity with the reduction of Mn^{III} by glyoxylic acid.

3.2 *Equilibrium measurements*

The fast hydration/dehydration equilibria of glyoxylic acid and its conjugate base in water has been well-studied and discussed at length by Nayak *et al.*[19] The acid and its anion exist in the monohydrate form (gem-diol) to the extent of >99% and 93–95%, respectively. We, therefore, consider the protolytic equilibrium of HGl in terms of the gem-diols:

$$\underset{}{HC(=O)CO_2H} + H_2O \xrightarrow[H_2O]{\text{fast}} \underset{HGI\ (gem\text{-}diol)}{HC(OH)_2CO_2H} \overset{K_1}{\rightleftharpoons} \underset{GI^-\ (gem\text{-}diol)}{HC(OH)_2CO_2^-} + H^+$$

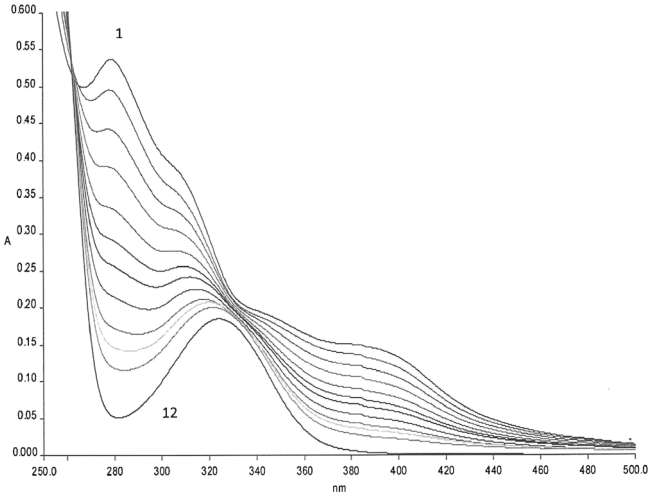

Figure 2. Repetitive spectral scans of the reaction mixture of $Mn^{III}(salen)(OH_2)_2^+$ + glyoxylic acid at 40°C. $[complex]_T = 2.855 \times 10^{-5}$, $[Gl]_T = 0.08$ mol dm^{-3}, pH = 2.05; time in minutes (curve no.): 0(1), 7 (2), 18 (3), 31(4), 48 (5), 63 (6), 79 (7), 101 (8), 131 (9), 166 (10), 216 (11), 1440 (12).

so that $[Gl^-] = f_1[Gl]_T$, $[HGl] = f_2[Gl]_T$ where $f_1 = K_1/([H^+] + K_1)$, $f_2 = [H^+]/([H^+] + K_1)$ and $[Gl]_T = [HGl] + [Gl^-]$. The acid dissociation constant (pK_1) of HGl was determined by pH titration. We obtained pK_1 =3.01 ± 0.05 at 28.0°C and $\boldsymbol{I}$ = 0.3 mol dm^{-3} in satisfactory agreement with the reported values (lit. values : pK_1 = 2.98–3.46, $0 \leq \boldsymbol{I}$ / mol dm^{-3} $\leq$ 1.0, 20–25°C; ΔH/kJ mol^{-1} = −2.51).[22,23]

There was a small but measurable instantaneous spectral change (ΔA) (see figure 3) at 280–320 nm for the mixture of $Mn^{III}(salen)(OH_2)_2^+$ + HGl relative to that of the sum of the absorbance of the complex and HGl at the same pH indicating fast complex formation between the two. At constant $[Mn^{III}(salen)(OH_2)_2^+]$ (6.00×10^{-5} mol dm^{-3}), varying $[Gl]_T$ (0.005–0.15 mol dm^{-3}) ($\boldsymbol{I}$ = 0.3 mol dm^{-3}), virtually constant pH (4.34–4.09) at which HGl exists predominantly as Gl^-, the equilibrium (4) is valid.

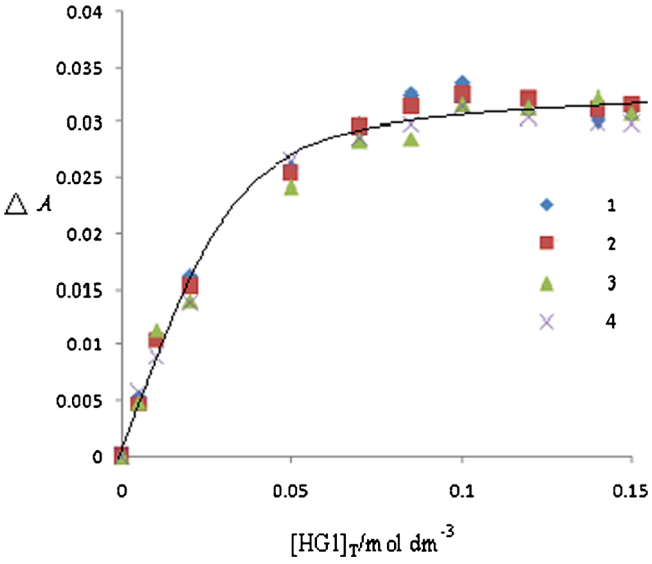

Figure 3. ΔA versus $[Gl]_T$/ mol dm^{-3} plot at 280.1 (1), 290.2 (2), 310.3 (3), and 319.9 nm (4); 4.34 ≤ pH ≤ 4.01, $[Mn^{III}(salen)(OH_2)_2^+]_T = 6.0 \times 10^{-5}$, $\boldsymbol{I}$ = 0.3 mol dm^{-3}, 27 ± 1°C.

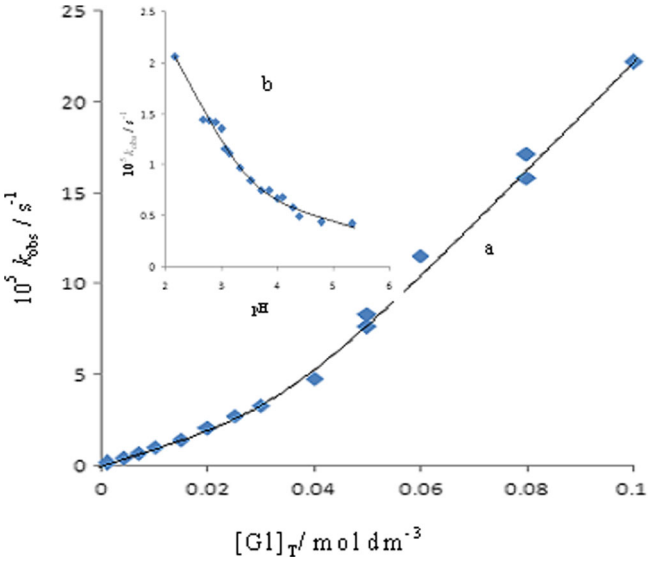

Figure 4. $10^5\ k_{obs}$ / s^{-1} vs. $[Gl]_T$ /mol dm^{-3} plot, 40°C, pH = 2.13 ± 0.27; (b inset) $10^5 k_{obs}$/s^{-1} vs. pH plot, $[Gl]_T$ = 0.02 mol dm^{-3}, 45°C.

$$Mn^{III}(salen)(OH_2)_2^+ + Gl^- \overset{K_M}{\rightleftharpoons} Mn^{III}(salen)(OH_2)(Gl)\,. \quad (4)$$

The absorbance data ($\Delta A = A_{GIT} + A_{MnIII} - A_{mixedsolution}$), analysed by equation (5) under the

$$\frac{c}{\Delta A} = (\Delta\varepsilon)^{-1} + (\Delta\varepsilon K_M)^{-1} \times (f_1\,[Gl]_T)^{-1}\,, \quad (5)$$

condition, $[Gl]_T >>> c$, where $c = \left[Mn^{III}(salen)(OH_2)_2^+\right]_T$, $\Delta\varepsilon = \varepsilon_1 - \varepsilon_2$, ε_1 and ε_2 being the molar extinction coefficients of $Mn^{III}(salen)(OH_2)_2^+$ and $Mn^{III}(salen)(OH_2)(Gl)$, respectively, yielded $10^3(\Delta\varepsilon)^{-1}$/mol dm^{-3} cm and $10^5(\Delta\varepsilon\ K_M)^{-1}$ /mol^2 dm^{-6} cm as (1.378 ± 0.11), (4.78 ± 0.15) (280.1 nm); (1.226±0.18), (5.521±0.25) (290.2 nm); (1.534 ± 0.089), (3.046 ± 0.12) (310.3 nm); (1.617 ± 0.119), (4.541 ± 0.016) (319.9 nm) (Corr. Coeff. 0.992–0.996), respectively. The weighted average value of K_M turned out as 33.2±5.3 dm^3 mol^{-1}.

3.3 *The slow reaction of HGl with $Mn^{III}(salen)(OH_2)_2^+$*

The slow reaction of HGl with $Mn^{III}(salen)(OH_2)_2^+$ was identified as redox reaction (see experimental section) succeeding the initial fast equilibrium complexation of $Mn^{III}(salen)$ by HGl/Gl$^-$. The pseudo-first order rate constants (k_{obs}) at varying $[HGl]_T$, pH (1.83–6.10) and temperatures (30–45°C) are presented in tables 1 and 2. Figure 4(a) displays the variation of $k_{obs}$with [HGl] at constant pH (= 2.13±0.27) at 45.0°C. A clear cut evidence for the greater than first order dependence of k_{obs} on $[HGl]_T$ (at constant pH 2.13) emerges. Similar trend is observed at other temperatures. Under this condition, the major reductant species is HGl (88%). However, k_{obs} at constant $[Gl]_T$ (=0.02 mol dm^{-3}) reflects a steadily decreasing trend with the increase of pH at all temperatures (see figure 4b, inset). This indicates that Gl$^-$, in contrast to our expectations, is not a superior reducing agent (kinetically) than its conjugate acid, HGl. This trend is rarely reported in the literature. Interestingly, reduction of Mn^{IV} in $[Mn_3^{IV}(\mu\text{-}O)_4(Phen)(OH_2)_2]^{4+}$ (Phen = 1,10 ortho phenanthroline) by glyoxylate follows a similar trend as reported by Mandal *et al.*[24], Das *et al.*[25] interpreted the observed increasing trend of k_{obs} with decreasing pH for the reduction of a Mn^{IV} tetramer $[Mn_4(\mu\text{-}O)_6(bipy)_6]^{5+}$ (bipy = 2,2′ bipyridyl) in terms of relatively higher reactivity of the protonated form of the complex with HGl. In another recent study of oxidation of glyoxylic by *tris*(biguanide)manganese(III) ($[(big)_3Mn^{III}]^{4+}$), Dhar *et al.*[26] report that it is the acid form, HGl, which has kinetic significance in the redox process but not the conjugate anion, Gl$^-$.

Under our experimental conditions the dissociation of the di-aqua complex, $Mn^{III}(salen)(OH_2)_2^+$ to the corresponding (aqua) (hydroxo) form can be neglected {$pK_{MnIII(salen)(OH2)2}$ = 7.7(10°C), 7.4 (25°C) $\boldsymbol{I}$ = 0.3 mol dm^{-3} [10]; 7.79, 7.34 (kinetic data) at 30°C, $\boldsymbol{I}$ = 0.2 mol dm^{-3}}.[15] Further, its absorption spectrum in moderately acidic media ($10^{-5} \le [H^+]$/ mol dm^{-3} ≤ 0.1, figure S1) is essentially acid independent indicating thereby that the complex does not undergo

protonation at least up to pH 1. The plausible reactions in tune with these observations are depicted in scheme 1.

Accordingly k_{obs} is given by equation (6) where

$$k_{obs} = \frac{k_0 Q_1 f_1 [Gl]_T + k_1 Q_2 f_2 [Gl]_T + k_2 Q_1 f_1^2 [Gl]_T^2 + k_3 Q_2 f_2^2 [Gl]_T^2 + k' f_1 f_2 [Gl]_T^2}{1 + Q_1 (f_1 + R f_2) [Gl]_T}$$

$$k' = k_4 Q_1 + k_5 Q_2, \qquad (6)$$

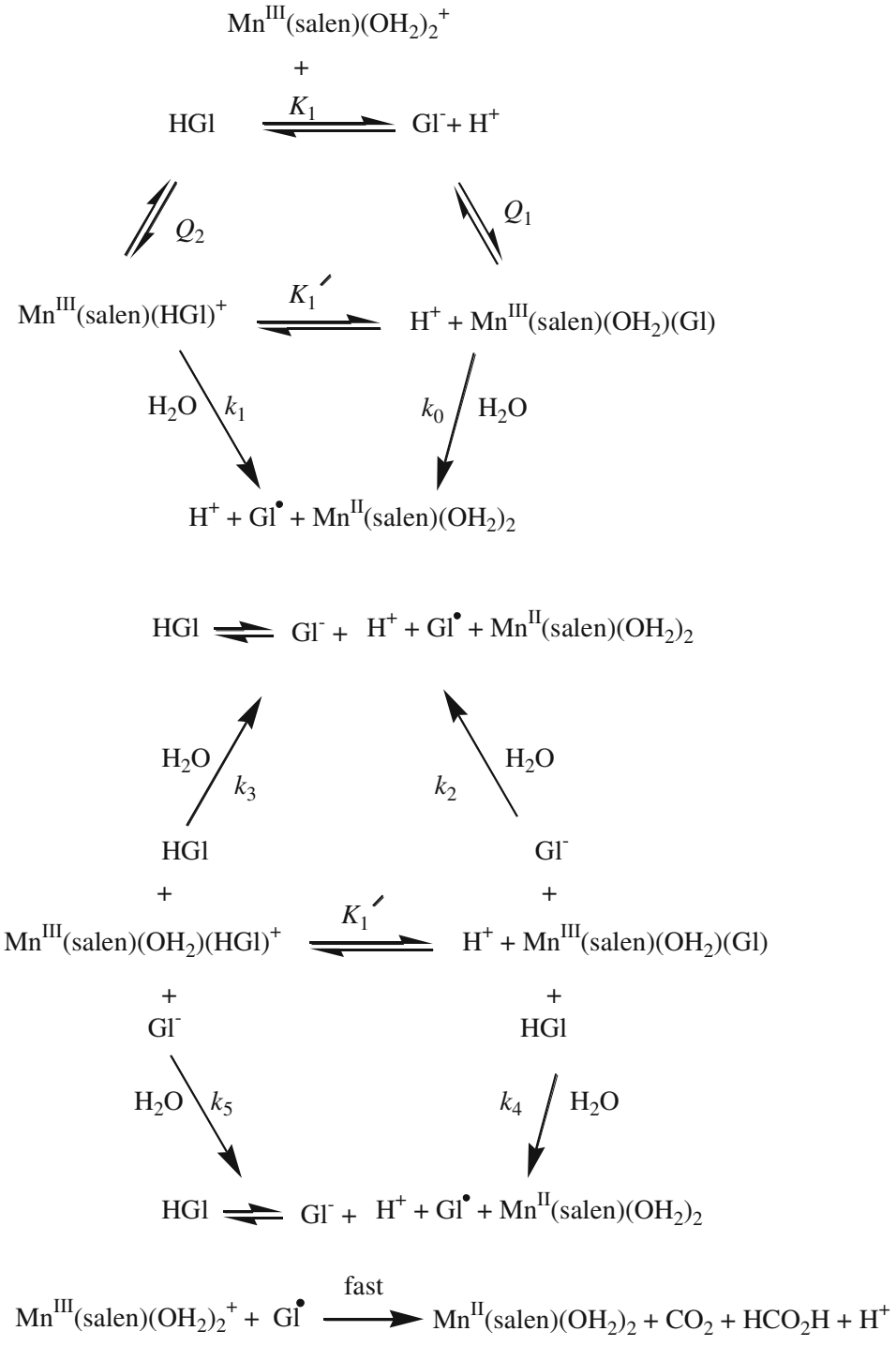

Scheme 1. Reduction of $Mn^{III}(salen)(OH_2)_2^+$ by glyoxylate species, $HC(OH)_2CO_2H$ (HGl) and $HC(OH)_2CO_2^-$ (Gl^-).

$R = Q_2/Q_1$; f_1, f_2 , $[Gl]_T$ are as mentioned earlier and all other terms are as defined in scheme 1 (note k_i (corr.) = $k_i/2$, 2 stands for stoichiometry, subscript i = 0–5).

3.4 *Analysis of the rate data (k_{obs})*

The rate constants (k_{obs}) are fitted to equation (6) by a nonlinear least squares program by varying all the parameters with the restriction that the value of R (= Q_2/Q_1) is < 1 and pK_1 (= 3.0 at $30.0 \leq t/°C \leq 45.0$) is temperature independent (reflected by the low value of the associated ΔH, see above). The calculated rate parameters are given in table 3. It is evident that both the terms, k_0Q_1 and k' are statistically insignificant (see table 3).

The relevant activation parameters obtained by weighted least squares fit of k_is ($w_i = (1/\sigma_{ki})^2$) to the Eyring equation, $k_i = (k_BT/h) \exp\left(-\Delta H^{\neq}/RT + \Delta S^{\neq}/R\right)$ are also collected in table 3. A comparison of k_{cal} with k_{obs} (see tables 1 and 2) shows the validity of equation (6) in relation to the proposed scheme. Neglecting the (k_0Q_1) and k' terms the representative plots of $10^5\left[k_{obs}(1 + Q_1(f_1 + Rf_2)[Gl]_T) - k_2Q_1f_1^2[Gl]_T^2\right] / (f_2[Gl]_T)$ vs. $10^2 f_2[Gl]_T$ (see figures S2 and S3) at 30°C and 45°C for the linearized form of equation (6) also bear this fact.

3.5 *Effect of ionic strength on k_{obs}*

The reaction is relatively complex in the sense that it involves several rate and equilibrium steps. As such a detailed analysis of ionic strength effect is not attempted. However, limited rate measurements are reported at pH = 2.23 ± 0.07, $[Gl]_T = 0.020$ mol dm^{-3} (40°C) and $0.01 \leq \boldsymbol{I}$ / mol dm^{-3} ≤ 0.4. Under this condition >85% of $[Glyoxalic\ acid]_{total}$ exists in the form of HGl. We observe a small rate retardation of the overall rate with the increase of ionic strength {10^5 $k_{obs}/s^{-1}(\boldsymbol{I}$, mol dm^{-3}) = 1.57 (0.01), 1.49(0.02), 1.41 (0.05), 1.35 (0.10), 1.29 (0.20), 1.30 (0.30), 1.15 (0.40)} consistent with involvement of oppositely charged ions (see scheme 1).

3.6 *Molecular modelling and structure optimization*

The ground state geometries of all the complexes were optimized using density functional theory (DFT). The BP86 functional and def2-TZVPP basis set within the resolution-of-the-identity (RI) approximation[27,28] (RI-BP86/def2-TZVPP in short) was employed for the optimization procedure. Frequency calculations of the optimized structures were done to ensure that they were true minima not the transition states. The DFT calculations were accomplished with the TURBOMOLE program package (Version-6.4).[29] The 'freeh' script of turbomole was used to calculate the free energies. The free energies of the complexes were computed at 25°C (298 K) and 1 atmospheric pressure. For the graphical presentation and the bond distance and angle measurements Mercury 3.0 was used.[30]

3.7 *Analysis of results*

Our results indicate that internal electron transfer from the coordinated glyoxylate to Mn^{III} in Mn^{III}(salen)(OH_2)(Gl) is not a favourable process as compared to the same for its conjugate acid analogue,

Table 3. Calculated rate and equilibrium constants.[a,b]

Parameters	30.0 ± 0.1°C	35.0 ± 0.1°C	40.0 ± 0.1°C	45.0 ± 0.1°C	$\Delta H^{\neq}$ / kJ mol^{-1}	ΔS^*/J K^{-1} mol^{-1}
$10^5 k_0Q_1$/dm^3 mo^{-1} s^{-1}	0.064 ± 12.3	0.82 ± 5.54	0.56 ± 7.73	0.93 ± 9.60	–	–
$10^2 k'$/ dm^6 mol^{-2} s^{-1}	0.032 ± 0.01	1.27 ± 0.50	0.12 ± 0.50	0.24 ± 0.77		
$10^5 k_1Q_2$ / dm^3 mo^{-1} s^{-1}	38.1 ± 10.1	54.6 ± 5.2	60.1 ± 5.0	62.0 ± 9.8		
$10^3 k_2Q_1$ / dm^6 mol^{-2} s^{-1}	5.87 ± 7.07	8.60 ± 2.93	14.15 ± 4.40	21.7 ± 5.4		
$10^2 k_3Q_2$/ dm^6 mo^{-2} s^{-1}	2.54 ± 0.15	2.80 ± 0.09	2.61 ± 0.07	3.89 ± 0.15		
$Q_1(Q_2)^c$/ mol dm^{-3}	33.0 (19.8)	33.0 (19.8)	25.0 (10.0)	18 (7.2)	–	–
R	0.6	0.6	0.4	0.4		
$10^5 k_0$/s^{-1}	0.002 ± 0.37	0.025 ± 0.17	0.022 ± 0.31	0.051 ± 0.53		
$10^5 k_1$ / s^{-1}	1.92 ± 0.51	2.76 ± 0.26	6.01 ± 0.50	8.61 ± 1.36	93 ± 11	−28 ± 36
$10^4 k_2$ / dm^3 mol^{-1} s^{-1}	1.78 ± 2.14	2.61 ± 0.88	5.66 ± 1.76	12.05 ± 3.04	119 ± 6	+75 ± 20
$10^3 k_3$ / dm^3 mol^{-1} s^{-1}	1.28 ± 0.08	1.41 ± 0.05	2.61 ± 0.07	5.40 ± 0.21	93 ± 18	+3 ± 60
$10^4 k_4$ / dm^3 mol^{-1} s^{-1}[d]	0.06 ± 0.02	2.4 ± 0.95	0.34 ± 1.4	0.96 ± 3.0		
F [e]	2.10	0.76	1.42	4.96		

[a] $\boldsymbol{I}$ = 0.3 mol dm^{-3}. [b] errors of (k_0Q_1) and k' estimated after fixing the values of other parameters and vice versa. [c] $Q_2 = R \times Q_1$. [d] $k_4 = k_5 = k'/(Q_1 + Q_2)$. [e] $F = \sum\left[10^5 (k_{cal} - kobs)\right]^2$

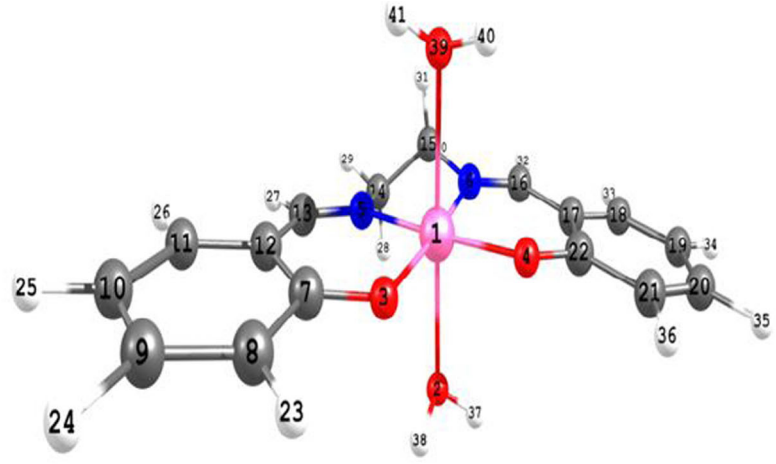

(A)

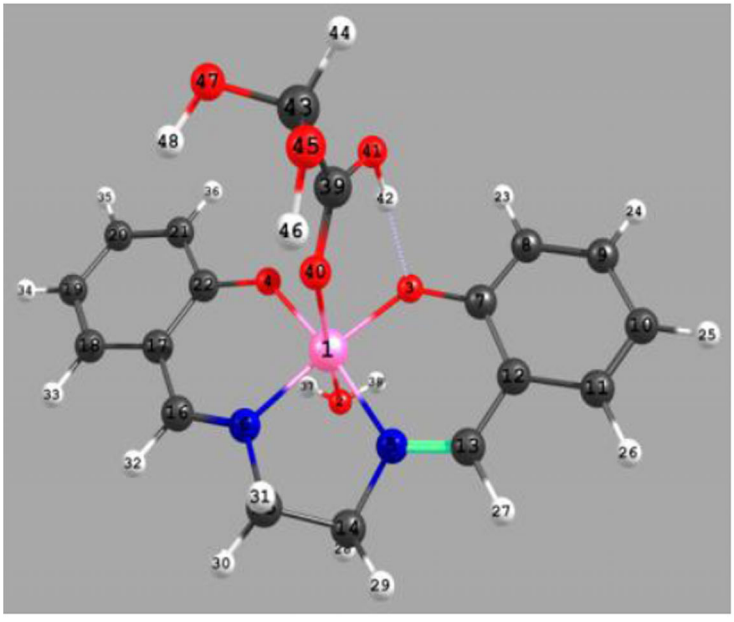

(B)

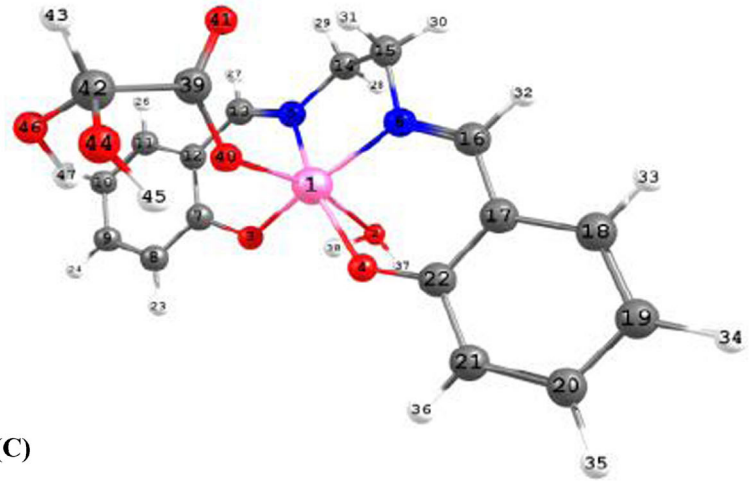

(C)

Figure 5. RI-BP86/def2-TZVPP optimized structures of Mn^{III}(salen)$(OH_2)_2^+$ (**A**), Mn^{III}(salen)$(H_2O)(HGl)^+$ (**B**) and Mn^{III}(salen)(H_2O)(Gl) (**C**) with atom labelling, **1** denotes Mn^{III}.

Table 4. Selected bond distances (Å) and bond angles (deg) for the RI-BP86/def2-TZVPP optimized structures of complexes, *trans*- $Mn^{III}(salen)(OH_2)_2^{+}$ (A), $Mn^{III}(salen)(OH_2)(HGl)^{+}$ (B), and $Mn^{III}(salen)(OH_2)(Gl)$ (C).

A	B	C
Bond distances		
Mn-O(2 W) 2.424	Mn-O(2 W) 2.466	Mn-O(2 W) 2.996
Mn-O(39 W) 2.424	Mn-O(40 O=C-OH) 2.353	Mn-O(40 $^{-}$O-C=O) 2.047
Mn-O(3 phenoxide) 1.880	Mn-O(3 phenoxide) 1.914	Mn-O(3 phenoxide) 1.914
Mn-O(4 phenoxide) 1.880	Mn-O(4 phenoxide) 1.868	Mn-O(4 phenoxide) 1.897
Mn-N(5 imine) 1.985	Mn-N(5 imine) 1.976	Mn-N(5 imine) 1.995
Mn-N(6 imine) 1.985	Mn-N(6 imine) 1.985	Mn-N(6 imine) 1.990
	O(3). . .H(42) 1.745	
Bond Angles		
O(2)-Mn-O(39) 176.5	O(2)-Mn-O(40) 175.7	O(2)-Mn-O(40) 164.8
O(3)-Mn-O(39) 90.4	O(3)-Mn-O(40) 87.5	O(2)-Mn-O(40) 96.2
O(4)-Mn-O(39) 87.1	O(4)-Mn-O(40) 89.4	O(4)-Mn-O(40) 99.2
N(5)-Mn-N(6) 82.6	N(5)-Mn-N(6) 82.9	N(5)-Mn-N(6) 82.2
O(4)-Mn-N(6) 90.8	O(4)-Mn-N(5) 91.4	O(4)-Mn-N(6) 90.7
O(3)-Mn-N(5) 90.8	O(3)-Mn-N(6) 91.4	O(3)-Mn-N(5) 89.4
O(4)-Mn-N(5) 173.3	O(4)-Mn-N(5) 171.4	O(4)-Mn-N(5) 162.6
O(3)-Mn-N(6) 173.3	O(3)-Mn-N(6) 173.5	O(3)-Mn-N(6) 162.6
O(3)-Mn-O(4) 95.8	O(3)-Mn-O(4) 94.6	O(3)-Mn-O(4) 93.1
O(3)-Mn-O(2) 87.3	O(3)-Mn-O(2) 89.4	O(3)-Mn-O(2) 68.7
O(4)-Mn-O(2) 90.4	O(4)-Mn-O(2) 87.9	O(4)-Mn-O(2) 81.3
N(5)-Mn-O(39) 93.5	N(6)-Mn-O(40) 97.0	N(6)-Mn-O(40) 100
N(6)-Mn-O(39) 89.2	N(5)-Mn-O(40) 90.2	N(6)-Mn-O(2) 95.2
Mn-N(6)-C(15) 113.2	Mn-N(6)-C(13) 124.7	Mn-N(5)-C(13) 124.7
Mn-O(4)-C(22) 130.6	Mn-O(4)-C(22) 131.5	Mn-O(4)-C(22) 131.2
Mn-O(3)-C(7) 130.6	Mn-O(3)-C(7) 130.0	Mn-O(3)-C(7) 126.1

$Mn^{III}(salen)(H_2O)(HGl)^{+}$ (i.e., $k_0 << k_1$). The values of Q_1 and Q_2, however, reflect that HGL forms a much weaker complex than GL^{-} with $Mn^{III}(salen)^{+}$. Thus the redox activity is inversely related to the thermodynamic stability. The nature of the two complexes can be judged considering the outer-sphere association of Gl^{-} and HGl with $Mn^{III}(salen)(OH_2)_2^{+}$ on statistical considerations and theory of diffusion[31,32] according to which

$$Q_{out} = \left(4\pi Na^3/3000\right) \exp(b) \exp\left[-bk_p a/\left(1 + k_p a\right)\right], \quad (7)$$

where $b = |Z_1 Z_2| e^2/DaK_B T$, a is the distance (cm) of closest approach between the participating species carrying charges Z_1 and Z_2, e is electronic charge (esu), D is the bulk dielectric constant of the medium, k_B is the Boltzmann constant (ergs), $k_p \left(= \left[\left(8\pi Ne^2/1000DK_B T\right) I\right]^{1/2}\right)$ is the Debye Huckel ion atmosphere parameter and T is the absolute temperature. At 25°C the calculated values of Q_{out}, using a constant value of $a = 5$ Å ($I = 0.3$ mol dm^{-3}), are 0.7 and 0.3 dm^3 mol^{-1} for $Mn^{III}(salen)(OH_2)_2^{+}$, Gl^{-} and $Mn^{III}(salen)(OH_2)_2^{+}$, HGL, respectively which are very much lower than the corresponding values obtained from the equilibrium study and kinetic data fitting (see table 3). This supports the inner sphere nature of such complexes which are believed to be generated by replacement of the coordinated H_2O by HGL and Gl^{-}. We have made structural characterization of these adducts (inner sphere complexes) along with the corresponding diaqua complex, $Mn^{III}(salen)(OH_2)_2^{+}$, by a computational study (see figure 5). Some selected bond distances (Å) and bond angles (deg) for the optimized structures of *trans*-$Mn^{III}(salen)(OH_2)_2^{+}$ (**A**), $Mn^{III}(salen)(OH_2)(HGl)^{+}$ (**B**), and $Mn^{III}(salen)(OH_2)(Gl)$ are given in table 4.

Notable fact is that there is no hydrogen bonding of the OH groups of the gem-diol moiety and Gl^{-} acts as a mono dentate ligand for the metal centre. Contrastingly, the HGl moiety binds $Mn^{III}(salen)$ virtually as a bi-dentate ligand, with one bond to Mn^{III} via the $-C = O$ function and the other via a hydrogen bond involving the carboxyl proton and the bound phenoxide {O(3). . .H(42) in figure 5B, *H-bond distance* = 1.745 Å, see table 4}. This imparts substantial thermodynamic stability to the complex, $Mn^{III}(salen)(OH_2)(HGl)^{+}$as reflected by the value of Q_2. A simple calculation shows that the acid dissociation constant of the coordinated HGl ($K_1' = K_1 Q_1/Q_2$) is only marginally (<10 times) higher than that of free

HGl. This is attributed to the locking of the acidic proton in the hydrogen bond.

The optimized structures and the computed structure parameters (i.e., bond distances and bond angles) for the complexes, *trans*-$Mn^{III}(salen)(OH_2)(X)$ (X=H_2O, HGl, G^-) are provided in tables S1, S2 and S3 (supplementary information). Mn^{III} is tightly held by the salen scaffold being slightly displaced above the plane of N,N(imines) and O,O (phenoxides) (~0.03 Å for $Mn^{III}(salen)(OH_2)(HGl)^+$, and ~0.27 Å for $Mn^{III}(salen)(H_2O)(Gl)$). Significant axial distortion is noted for these two complexes (see table 4). A comparison of the Mn^{III}-X bond length *trans* to the Mn^{III}-OH_2 in the complexes, $Mn^{III}(salen)(H_2O)(X)$: 2.6209 [15], 2.424, 2.353, 2.407 Å and similarly the Mn^{III}-OH_2 bond length *trans* to Mn^{III}-X: 2.3329 [15], 2.424, 2.466, and 2.996 Å for X = Cl^-, H_2O, HGl and Gl^-, respectively demonstrates that the ground state structural *trans* effect (GSTE) is the strongest for $Mn^{III}(salen)(H_2O)(Gl)$. However, the Mn^{III}-O(phenoxide) and Mn^{III}-N(imine) bonds in all such complexes (see ref. 15 and table 4) do not reveal substantially different axial ligand dependent distortion of the N_1,N_2,O_1,O_2 square plane. In order to assess how the GSTE influences the equilibria involving the replacement of the second water molecule from *trans* $Mn^{III}(salen)(OH_2)(Gl/HGl)^{0/+}$ by Gl^-/HGl (Eqs 8, 9),

$$Mn^{III}\,(salen)\,(OH_2)\,(Gl) + Gl^- \overset{Q_3}{\rightleftharpoons} Mn^{III}\,(salen)\,(Gl)^- + H_2O, \quad (8)$$

$$Mn^{III}\,(salen)\,(OH_2)\,(HGl)^+ + HGl- \overset{Q_4}{\rightleftharpoons} Mn^{III}\,(salen)\,(HGl)_2^+ + H_2O. \quad (9)$$

We made an attempt to compute theoretically the relevant ΔG^0 values at 25°C. ΔG^0 for equilibrium (8) turned out negative (~$^-$79.5 kJ mol^{-1}) while the same for (9) was positive (~8.6 kJ mol^{-1}). This goes in favour of inner sphere binding of Gl^- (Eq. 8) but not HGl in the second step despite relatively *stronger ground state structural trans* effect of Gl^-. We must mention here that the equilibria (8) and (9) could not be detected under the experimental conditions. However, our computational strategy attempts to differentiate the mechanistic path ways of reduction of $Mn^{III}(salen)(OH_2)(Gl)$ by Gl^- and $Mn^{III}(salen)(H_2O)(HGL)^+$ by HGL; the former involves inner sphere mechanism unlike the latter for which the outer sphere mechanism might prevail (k_2 and k_3 paths in scheme 1).

A comparison of the rate constants (k_is) given in table 3 shows that the intra molecular reduction of Mn^{III} in $Mn^{III}(salen)(OH_2)(Gl)$ (k_0 path) is statistically insignificant as for $Mn^{III}(salen)(OH_2)(HQ)$ and $Mn^{III}(salen)(OH_2)(Hcat)$ (H_2Q and H_2cat denote hydroquinone and catechol, respectively)[15] and $Mn^{III}(salen)(H_2O)(SO_3)^{-10}$ while the same for $Mn^{III}(salen)(OH_2)(HGl)^+$ is moderately facile (k_1 path); both steps are likely to involve inner sphere mechanism as electron transfer occurs through the bound ligands, Gl^- and HGl. For the k_1 path $\Delta H^{\neq}$ is substantially high and $\Delta S^{\neq}$ is close to zero (or small negative, see table 3) as expected for an intra molecular process with some degree of bond rearrangement. Further, the observed differential rates (k_1 vs k_0), and the activation parameter data make us inclined to think that *H-bond* in $Mn^{III}(salen)(OH_2)(HGl)^+$ as also the net positive charge at the Mn^{III} centre play a dominant role to consider this 'electro-protic reaction' as a distinct case of 'proton coupled electron transfer' process (see figure 6).

A comparison of the second order rate constants ($k_4 < k_2 < k_3$, see table 3) also reveals that HGl reduces much faster than Gl^- unlike in several other cases where reverse sequence has been reported for anions and their conjugate acids reducing various Mn^{III} complexes.[33]

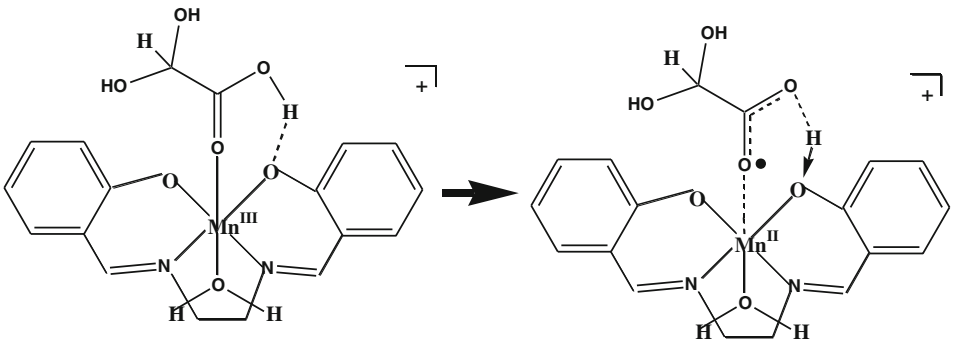

Figure 6. Proton coupled electron transfer in $Mn^{III}(salen)(OH_2)(HGl)^+$.

Interestingly, the results of Das and co-workers[25] are in agreement with ours where they show that glyoxylic acid (HGl) *very likely* reduces Mn^{IV} in $[Mn_4(\mu\text{-}O)_6(bipy)_6]^{4+}$ ($\mathbf{I}^{4+}$) appreciably faster than its conjugate anion (Gl^-) ($\mathbf{I}^{4+}+HGl \rightarrow$, $k_{red} > 50$ dm^3 mol^{-1} s^{-1} ; $\mathbf{I}^{4+} + Gl^- \rightarrow$, $k_{red} = 0.68$ dm^3 mol^{-1} s^{-1} at 25°C, I = 1.0 mol dm^{-3}). However, proton ambiguity in that case is a serious shortcoming as pointed out by them. The reduction of Mn^{IV} in $[Mn^{IV}_3(\mu\text{-}O)_4(Phen)(OH_2)_2]^{4+}$ by HGl/Gl^-have been shown by Mandal and co-workers[24] to follow second order kinetics with the reactivity trend, $k_{red}(HGl) > k_{red}(Gl^-)$, an observation similar to ours but for the proton ambiguity in their case. In a recent study of the oxidation of glyoxylic acid by $Mn^{IV}L$ and Mn^{III} L {L = tetra deprotonated 1,8-bis(2-hydroxybenzamido)-3,6-diazaoctane} Nayak and co-workers[19] have unambiguously demonstrated the higher reactivity of HGl relative to that of its conjugate base, Gl^- and attributed this reactivity order to the preferential hydrogen bonding effect of HGl.

The activation enthalpy for the k_2 path is marginally higher than the same for the k_3 path ($\Delta H^{\neq}(k_2) - \Delta H^{\neq}(k_3) = 26 \pm 19$ kJ mol^{-1}) and the corresponding difference in the activation entropy is also similar in magnitude ($\Delta S^{\neq}(k_2) - \Delta S^{\neq}(k_3) = +72 \pm 63$ J K^{-1} mol^{-1}). Our computational study shows that unlike HGl, Gl^- can still bind to Mn^{III} centre via H_2O replacement of $Mn^{III}(salen)(H_2O)(Gl)$ forming a precursor ($Mn^{III}(salen)(Gl)_2^-$) preceding electron transfer via inner sphere mechanism (k_2 path). Hence, in this case the overall activation enthalpy and entropy will have contributions from the equilibrium precursor formation and the redox step. On the contrary, no such inner sphere precursor complex between HGl and $Mn^{III}(salen)(H_2O)(HGl)^+$ appears to be formed preceding the electron transfer step via k_3 path. Hence it is not unlikely that the activation parameters for the k_2 and k_3 paths will differ by a small margin. However, the large values of $\Delta H^{\neq}$(93–119 kJ mol^{-1}) reflect substantial reorganization energy which is expected for inner sphere ET process.

4. Conclusion

The electron transfer reaction between glyoxylic acid and $Mn^{III}(salen)(OH_2)_2^+$ involves equilibrium pre-association of the reactants yielding inner-sphere complexes, $Mn^{III}(salen)(OH_2)(Gl)$ and $Mn^{III}(salen)(OH_2)(HGl)^+$, where HGl and Gl^- are the gem-diols of the acid and the conjugate base forms of the reductant, respectively. Computational study shows that the proton of the carboxylic acid function is hydrogen bonded to one of the coordinated phenoxide function while both the diol-OH groups are not involved in H-bonding in the state of coordination of HGl and Gl^- to Mn^{III}. There is remarkable kinetic stability of $Mn^{III}(salen)(H_2O)(Gl)$ towards intra-molecular electron transfer in contrast to moderate rate of intra-molecular reduction of Mn^{III} centre by the coordinated HGl. This electro-protic reaction through the influence of H-bond, is considered to be a clear case of 'proton coupled intra-molecular electron transfer' process. However, $Mn^{III}(salen)(H_2O)(Gl)$ further undergoes reduction of Mn^{III} centre by Gl^- in a second order process as also $Mn^{III}(salen)(H_2O)(HGl)^+$ by HGl; computational study, however, indicates the possibility of adduct formation between $Mn^{III}(salen)(OH_2)(Gl)$ and Gl^- but not between $Mn^{III}(salen)(OH_2)(HGl)^+$ and HGl. We conclude that the intimate reduction steps follow inner-sphere mechanism possibly except in the second order path of the reaction between $Mn^{III}(salen)(OH_2)(HGl)$ and HGl.

Supplementary information

Figure S1 showing the lack of $[H^+]$ dependence of the Uv-Vis absorption spectra of $Mn^{III}(salen)(OH_2)_2^+$(pH = 1 – 4); figures S2 and S3 showing the plots of $10^5[k_{obs}(1+Q_1[Gl]_T(f_1+f_2R) - k_2Q_1f_1^2[Gl]_T^2]/(f_2[Gl]_T)$ $(=Y)$ vs. $10^2f_2[Gl]_T$ at 30°C and 45°C, respectively; Tables S1, S2 and S3 presenting the optimized structures and corresponding bond distances and bond angles for $Mn^{III}(salen)(OH_2)_2^+$ (**A**), $Mn^{III}(salen)(OH_2)(HGl)^+$ (**B**), and $Mn^{III}(salen)(OH_2)(Gl)$ (**C**), respectively are provided as supplementary materials (see www.ias.ac.in/chemsci).

Acknowledgements

Financial support from the University Grants Commission (UGC), New Delhi in terms of a Teacher Fellowship to AKK (Ref. T.F.OU3-007-1/10-11 (ERO)) is acknowledged. AKK thanks the Odisha Education Department and the authority of Sishu Ananta Mahavidyalaya, Khurda, Odisha, India for granting study leave. Authors thank Prof. Gautam K Lahiri, Indian Institute of Technology, Mumbai for ESR measurement. We also thank Dr. Himansu S Biswal, School of Chemical Sciences, National Institute of Science Education and Research (NISER), Bhubaneswar for the quantum chemical calculations and discussions.

References

1. Armstrong A F 2008 *Phil. Trans. R. Soc. B* **363** 1263
2. Brudvig G W 2008 *Phil. Trans. R. Soc. B* **363** 1211
3. Betley T A, Surendranath Y, Childress M V, Alliger G E, Ross F, Cummins C C and Nocera D G 2008 *Phil. Trans. R. Soc. B* **363** 1293 and references cited therein
4. McEvoy P J, Gascon A J, Batista S V and Brudvig G W 2005 *Photochem. Photobiol. Sci.* **4** 940
5. Berends H-M, Manke A-M, Näther C, Tuczek F and Kurz P 2012 *J. Chem. Soc. Dalton. Trans.* **41** 6215
6. (a) Noritke Y, Umezawa N, Kato N and Higuchi T 2013 *Inorg. Chem.* **52** 3653; (b) Lanza V and Vechhio G 2009 *J. Inorg. Biochem.* **103** 381; (c) de Boer J W, Browne W R, Feringa B L and Hage R 2007 *C. R. Chimie*. **10** 341; (d) Sharpe M A, Ollosson R, Stewart V C and Clark J B 2001 *Biochem. J.* **366** 97
7. Pecoraro V L, Gelasco A and Baldwin M J 1996 *Mechanistic bioinorganic chemistry*, (eds) Thorp H and Pecoraro V L *Advances in Chemistry, ACS Publication* **vol 26**, chapt. 10, pp 265; DOI: 10.1021/ba-1995-0246
8. Gunter T E, Miller L M, Gavin C E, Eliseev R, Salter J, Buntinas L, Alexandrov A, Hammond S and Gunter K K 2004 *J. Neurochem.* **88** 266
9. (a) Katsuki T 1995 *Coord. Chem. Rev.* **140** 189; (b) Young K J, Takase M K and Brudvig G W 2013 *Inorg. Chem.* **52** 7615
10. Dash A C and Das A 1999 *Int. J. Chem. Kinet.* **31** 627
11. (a) Nayak S and Dash A C 2005 *Transit. Met. Chem.* **30** 560; (b) Nayak S and Dash A C 2006 *Transit. Met. Chem.* **31** 316
12. Nakada H I, Friedmann B and Weinhouse S 1955 *J. Biol. Chem.* **216** 583
13. (a) E H Rodd 1952 *Chemistry of carbon compounds*, Elsevier, Amsterdam **vol 1** p 850; (b) Millered A, Morton R K and Wells J R E 1963 *Biochem. J.* **86** 57
14. (a) Ashmawy F M, McAuliff C A, Parish R V and Tames J 1985 *Inorg. Chim. Acta.* **103** 133; (b) Boucher L J and Farrell M O 1974 *J. Inorg. Nucl. Chem.* **36** 531
15. Panja A, Shaikh N, Ali Mahammad, Vojtišek P and Banerjee P 2003 *Polyhedron* **22** 1191
16. Dash A C and Nanda R K 1974 *Inorg. Chem.* **13** 655
17. Irving H M, Miles M G and Petit L D 1967 *Anal. Chim. Acta* **38** 475
18. Kramer D N, Klein N and Baselice R A 1959 *Anal. Chem.* **31** 250
19. Nayak S, Brahma G S, Reddy K Venugopal, Reddy K Veera and Dash A C 2011 *Polyhedron* **30** 1637
20. Feigel F 1956 *Spot Tests in organic analysis* (London: Elsevier) pp 331
21. Jordan D E 1980 *Anal. Chim. Acta* **113** 189
22. Martell A E and Smith R M 1977 *Crtical stability constants plenum*, New York **vol 3** pp 65
23. Kerber C and Fenando M S 2010 *J. Chem. Educ.* **87** 1679
24. Mandal P C, Das S and Mukhopadhyay S 2010 *Int. J. Chem. Kinet.* **42** 323
25. Das S, Bhattacharya J and Mukhopadhyay S 2006 *Helv. Chim. Acta* **89** 1947
26. Dhar B B, Mukherjee R, Mukhopadhyay S and Banerjee R 2004 *Eur. J. inorg. Chem.* 4854
27. Christiansen O, Koch H and Jorgensen P 1995 *Chem. Phys. Lett.* **243** 409
28. Kohn A and Hattig C 2003 *J. Chem. Phys.* **119** 5021
29. Ahlrichs R, Bar M, Haser M, Horn H and Kolmel C 1989 *Chem. Phys. Lett.* **162** 165
30. Macrae C F, Bruno I J, Chisholm J A, Edgington P R, McCabe P, Pidcock E, Rodriguez-Monge L, Taylor R, van de Streek J and Wood P A 2008 *J. Appl. Cryst.* **41** 466
31. Fuoss R M 1958 *J. Am. Chem. Soc.* **80** 5059
32. Eigen M 1954 *Z Physik. Chem. (Frankfurt)* **1** 176
33. Gangopadhyay S, Ali M and Banerjee P 1994 *Coord. Chem. Revs.* **135/136** 399